3

Diffusive signaling between endothelial cells and pericytes can cause network collapse and subsequent sprouting

This chapter is based on:

Margriet M. Palm, Henri H. Versteeg and Roeland M.H. Merks, *Diffusive signaling between endothelial cells and pericytes can cause network collapse and subsequent sprouting* (in preparation)

background graphic: network formed with pericytes and endothelial cells interaction via the contact-dependent signaling scenario.

Abstract

Pericytes are perivascular cells that are responsible for the stabilization of small blood vessels. However, in certain *in vivo* systems; such as the mouse retina, central nervous system and tumors; pericytes are observed in developing blood vessels. This suggest that pericytes can also play an active role in angiogenesis. How pericytes and endothelial cells interact during angiogenesis remains unclear. Therefore, we combined *in vitro* vasculogenesis assays with computational modeling to study how pericytes affect endothelial cells and vice versa. With the experiments we can find what patterns endothelial cells and pericytes form together. Then, by varying the interactions between endothelial cells and pericytes included in the model, we can test which interactions could cause *in vitro* patterns.

In the vasculogenesis assay endothelial cells and pericytes initially formed a network. This network quickly collapsed into a blob from which new sprouts extended. In our model we can reproduce the network collapse when endothelial cells attract pericytes and vice versa via chemotaxis. Furthermore, when the chemoattractant for endothelial cells is secreted by endothelial cells adjacent to pericytes instead of pericytes, sprouts extend from the blobs. Thus, our study suggests that during angiogenesis endothelial cells and pericytes attract each other via secreted chemoattractants, and pericytes may regulate the chemoattractant secretion of endothelial cells.

3.1 Introduction

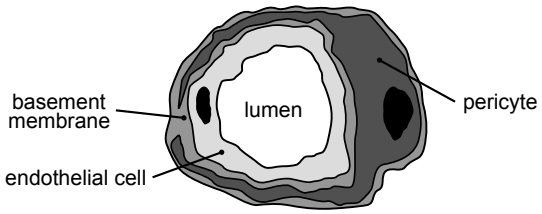

Figure 3.1: Schematic cross section of a small blood vessel.

The walls of small blood vessels, which the are arterioles, capillaries and venules, consist of endothelial cells and pericytes [97] (Figure 3.1). Endothelial cells form the inner layer of the vessel and this layer is covered with the endothelial basement membrane. Embedded in this membrane are the pericytes [98]. Pericytes are recruited to the walls of established blood vessels [99]. This pericyte recruitment is thought to stabilize blood vessels by stimulating the formation of the basement membrane [100] and inhibiting endothelial cell proliferation [101]. Several *in vivo* observations challenge the

view that pericytes are recruited to established vessels where they stabilize the vasculature. In the mouse retina and central nervous system, pericytes are integrated into the developing vessels [69, 70] and in tumor angiogenesis pericytes can lead sprouts [71], suggesting that pericytes interact actively with endothelial cells during blood vessel formation. However, most research focused on the role of pericytes in vessel stabilization and therefore the precise role of pericytes in blood vessel formation remains unclear. To clarify the role of pericytes in blood vessel formation we study how pericytes and endothelial cells interact. For this we combine *in vitro* experiments and computational modeling. By attempting to reproduce the patterns formed *in vitro* with a computational model we can reconstruct which cell behaviors could cause those patterns.

Pericytes and endothelial cells can signal over long distances via diffusive ligands, such as transforming growth factor-β (TGFβ), platelet-derived growth factor B (PDGFB), angiopoietin-1 (Ang-1), and vascular endothelial growth factor (VEGF). Juxtacrine signaling, via membrane-bound ligands and receptors, occurs for example via N-cadherin, and Jagged1 and Notch3 [97, 98, 102]. Endothelial-pericyte signaling regulates the behavior of pericytes and endothelial cells, the differentiation of pericytes and pericyte progenitors, and the maturation and stabilization of blood vessels. Because we are studying how endothelial cells and pericytes interact while forming blood vessels, we only consider the interactions that affect the migration of endothelial cells or pericytes and exclude interactions that only affect pericyte differentiation or vessel stabilization. Both the juxtacrine signaling pathways listed above are involved in vessel maturation and do not affect cell migration. This leaves the four diffusive ligands, which all affect endothelial cell or pericyte migration, as sources of endothelial-pericyte interactions. TGFβ is secreted by both pericytes and endothelial cells [103–105] in a latent form that must be chemically modified to become active [106]. This activation does not occur in pericyte or endothelial cell monocultures, but in endothelial-pericyte cocultures TGFβ is activated via an unknown mechanism [103–105]. In endothelial cells TGFβ regulates cell migration via activin receptor-like kinase (Alk)-1 and Alk-5 [98]. Alk-1 signaling promotes proliferation and migration while Alk-5 signaling inhibits these processes [107–109]. Because of the opposing effects of Alk-1 and Alk-5 signaling, the exact effect of TGFβ signaling on endothelial cell behavior remains unclear. In pericytes TGFβ signaling induces differentiation to vascular smooth muscle cells [110]. PDGFB is secreted by endothelial cells [111, 112] and is sensed by pericytes via PDGF receptor-beta (PDFGRβ) [111]. PDGFB-PDGFRβ signaling induces chemotaxis in pericytes [113] and thereby endothelial cells can attract pericytes. Ang-1 is secreted by pericytes and is sensed by endothelial cells via the receptor TIE2 [98]. This signaling induces chemotaxis in endothelial cells [114] and thereby causes pericytes

to attract endothelial cells. VEGF is sensed by endothelial cells via VEGF receptor 2 (VEGFR2) [115], which induces chemotaxis and promotes endothelial cell survival [116]. VEGF is suggested to play a role in endothelial-pericyte interactions because several studies showed that pericytes cocultured with endothelial cells secrete VEGF [117, 118]. However an alternative mechanism is suggested by Franco *et al.* [119] who showed that endothelial cells in contact with pericytes secrete VEGF. Franco *et al.* [119] proposed that VEGF secretion by endothelial cells is induced by the activation of membrane bound integrin α_V on endothelial cells by vitronectin that is secreted by pericytes. Thus, VEGF signaling attracts endothelial cells to pericytes, or to endothelial cells that are close to pericytes. Altogether, except for TGFβ, all diffusive ligands involved in endothelial-pericyte signaling induce chemotaxis in pericytes or endothelial cells.

Overall, based on the literature we propose that attraction via diffusive, secreted, ligands is a major mode of endothelial-pericyte interaction. Endothelial cells are known to secrete chemoattractants that attract pericytes, such as PDGFB, and pericytes secrete chemoattractants for endothelial cells, such as VEGF, Ang-1, and TGFβ. VEGF may be secreted by endothelial cells, in close vicinity of pericytes, instead of by pericytes. Thus, exactly via which chemoattractants pericyte and endothelial cells interact, and which cells secrete which chemoattractant remains unclear. Therefore, in this study we will use a computational model to find if attraction via chemotaxis between pericytes and endothelial cells plays a role during angiogenesis, and if so, which chemoattractant should be secreted by which cells. For this we first study pattern formation of endothelial cells and pericytes with vasculogenesis assays. Then, we try to reproduce these patterns with our computational, cell-based model. In such a model we can study how changes in cell behavior, such as chemotaxis and chemoattractant secretion, and the chemical properties of chemoattractants affect pattern formation. Thus, with our model we can search for the chemotaxis scenario that could cause the *in vitro* patterning.

3.2 Results

To study how endothelial cells and pericytes interact during blood vessel formation we used *in vitro* experiments in combination with computational models. For the *in vitro* experiments we used a standard vasculogenesis assay [45] in which cells are seeded on a substrate and the evolution of the pattern is monitored over time. We performed assays with only endothelial cells, only pericytes, or both pericytes and endothelial cells. Based on the results of the endothelial cells and pericytes monocultures we built a computational, cell-based model of endothelial cells and pericytes using the cellular Potts method and partial differential equations. The behavior of individual peri-

cytes and endothelial cells is chosen such that simulations with a single cell type correspond with the corresponding *in vitro* monocultures. Then, we used the model to study which endothelial-pericyte interactions may contribute to the patterns we observed in the *in vitro* endothelial-pericyte coculture. For this we assumed that endothelial cells and pericytes interact by secreting chemoattractants. For simplicity, we refer to the chemoattractant that endothelial cells secrete for pericytes as PDGFB, and we refer to the chemoattractant that pericytes secrete for endothelial cells as VEGF. However, these chemoattractants represent generic chemoattractants and therefore we did not use PDGFB and VEGF specific model parameters. For VEGF, it is debated whether it is secreted by pericytes [117, 118], or by endothelial cells that contact pericytes [119]. With a computational model we can simulate the tissues that develop based on each of these scenarios. For this, we set up two scenarios for endothelial-pericyte signaling: *paracrine signaling*, and *contact-dependent signaling*. In the paracrine signaling scenario, endothelial cells secrete a chemoattractant for pericytes and vice versa (Figure 3.2**A**). In the contact-dependent signaling scenario, we assumed that contact with pericytes induces VEGF secretion in endothelial cells [119]. Therefore, in this scenario PDGFB is secreted by all endothelial cells and VEGF is secreted by endothelial cells that are in contact with pericytes (Figure 3.2**B**).

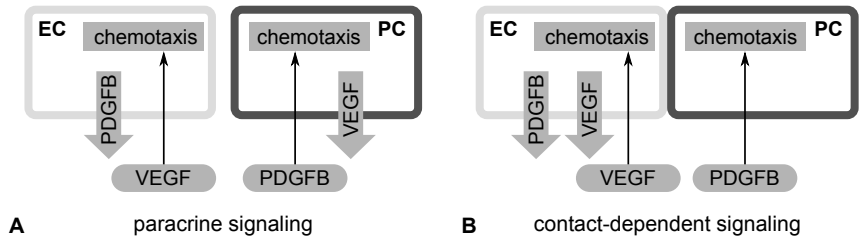

Figure 3.2: Alternative scenarios for endothelial-pericyte signaling.

3.2.1 *In vitro* patterning

We started with the *in vitro* experiments to elucidate what patterns form when endothelial cells and pericytes are seeded together. For this we seeded endothelial cells and pericytes, at a 2:1 ratio, and followed the pattern evolution. As a reference, we repeated the experiments with only endothelial cells, or only pericytes.

Figure 3.3 shows how the patterns evolved in each of the three assays. In the endothelial cell monoculture (Figure 3.3**A**) a network with long branches formed quickly. Between the second and eighth day the network disintegrated because the endothelial cells died. In the pericyte monoculture (Figure 3.3**B**)

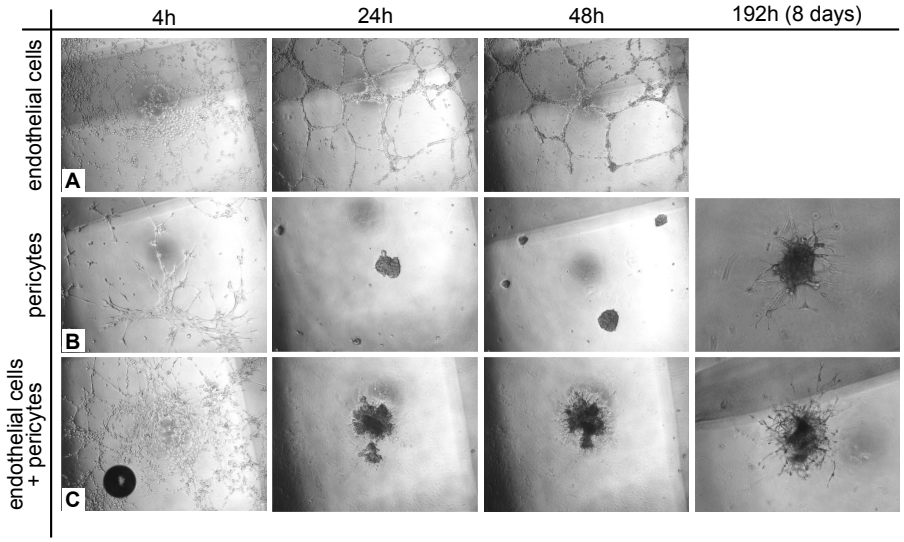

Figure 3.3: Pattern formation in vasculogenesis assays with endothelial cells (**A**), pericytes (**B**), or endothelial cells and pericytes at a ratio of 2:1 (**C**).

initially some branched structures formed that quickly collapsed into a blob. After eight days some sprouts extended from this blob. In the endothelial-pericyte coculture (Figure 3.3**C**) a network developed quickly. Within 24 hours, the network collapsed into a blob and later on sprouts extended from the blob. Comparing the evolution of a blob with only pericytes (Figure 3.3**B**) with that of a blob with pericytes and endothelial cells (Figure 3.3**C**) suggests that endothelial cells caused the sprouts to extend earlier and become longer. However, we currently lack quantitative data to support this conclusion.

Altogether, in all cultures networks formed quickly. However, when pericytes are present, the network collapsed to form a blob. Over time, sprouts extended from this blob, which seemed to be more numerous in the endothelial-pericyte coculture. These observations indicate that pericytes induce network collapse, and that endothelial cells may promote sprout formation from the cell blobs.

3.2.2 Modeling endothelial cells and pericytes

In our attempt to explain what endothelial-pericyte interactions cause the patterns observed in the *in vitro* coculture, we set out to develop a computational, cell-based model of endothelial-pericyte interactions. In this model we use the cellular Potts method (CPM) to model cells and partial differential equations (PDEs) to model chemoattractants. Cells are represented as groups of lattice sites $\vec{x} \in \mathbb{Z}^2$ on a square lattice identified by an identifier

$\sigma \in \mathbb{N}$. Each cell is associated with a type $\tau(\sigma) \in \{\text{EC,PC,ECM}\}$. To mimic cell motion the CPM iteratively attempts to move the cell membranes. Whether an attempt is accepted depends on the cell motility μ and the prescribed cell behaviors. The chemoattractant concentrations are projected on the same lattice as the cells. The concentration of a chemoattractant c at a site $\vec{x}$ is described with a PDE:

$$\frac{\partial c(\vec{x},t)}{\partial t} = D(c)\nabla^2 c(\vec{x},t) + \alpha(\tau(\sigma(\vec{x})),c) - \varepsilon(c);$$

with $c(\vec{x},t)$ the concentration of c, $D(c)$ the diffusion coefficient of c, $\alpha(\tau,c)$ the secretion rate of c by a cell of type τ, and $\varepsilon(c)$ the decay rate of c. The range over which a chemoattractant has spread in steady state ($\frac{\partial c(\vec{x},t)}{\partial t} = 0$) is characterized by the diffusion length: $\ell = \sqrt{\frac{D}{\varepsilon}}$, which is the distance from the chemoattractant source, where $c(\vec{x},t) = c_0$, at which the concentration has dropped to $\frac{c_0}{e}$. Note that, however, when a time step of the CPM is shorter than time needed for c to reach equilibrium, the chemoattractant will not diffuse as far as predicted.

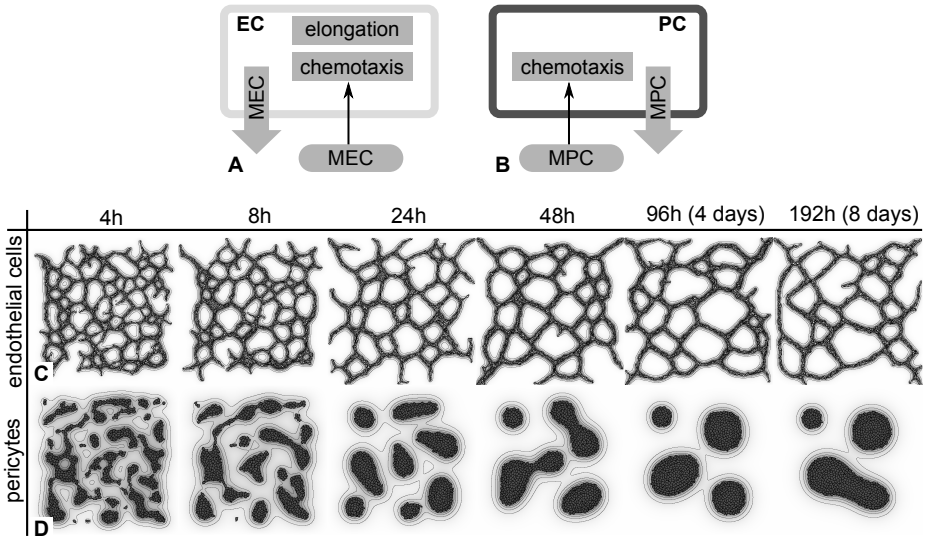

Figure 3.4: Models for endothelial cell and pericyte monocultures. **A** endothelial cells (ECs) elongate and secrete MEC that induces chemotaxis in endothelial cells. **B** pericytes (PCs) secrete MPC that induces chemotaxis in pericytes. **C**-**D** evolution of the pattern formed with 600 endothelial cells (**C**) or 600 pericytes (**D**).

The cell behaviors in the endothelial-pericyte model were prescribed such that a simulation with only pericytes or only endothelial cells results in a pattern similar to the pattern formed in the corresponding *in vitro* monocul-

ture. In the monoculture endothelial cells form networks with long branches. These networks are similar to the networks formed in a model with elongated cells that secrete their own chemoattractant [25]. Therefore, we modeled endothelial cells as elongated cells that secrete and chemotact towards a chemoattractant that we called "morphogen for endothelial cells" (MEC) (Figure 3.4**A**). Pericytes formed a network that quickly collapsed into a blob. This is similar to the evolution of a model with round cells that secrete their own chemoattractant [26, 28]. Thus, pericytes were modeled as round cells that secrete and chemotact towards a chemoattractant called "morphogen for pericyte" (MPC) (Figure 3.4**B**). For both endothelial cells and pericytes we fine-tuned the model parameters such that the pattern evolution was as close to the *in vitro* experiments as possible (Table 3.2), starting with the parameter values used in similar models [25, 28]. Figures 3.4**C** and **D**, and Movies S1 and S2, show the evolution of patterns formed by respectively endothelial cells and pericytes. The evolution of the pattern with endothelial cells is similar to the *in vitro* pattern evolution. The simulated pericytes initially form a network-like structure that collapses into multiple small blobs (Figure 3.4**D**). In the vasculogenesis assay a network formed and collapsed as well, but here a single blob formed (Figure 3.3**C**). Thus, our model does not exactly mimic the *in vitro* pattern formation, but it reproduces the phenomenology of the pericyte monocultures (Figure 3.3**C**).

endothelial-pericyte signaling is incorporated in the model by adding the chemoattractants VEGF and PDFGB. For *paracrine signaling* scenario PDGFB by all endothelial cells, and VEGF is secreted by all pericytes. For the *contact-dependent signaling* scenario PDGFB is again by all endothelial cells. But, VEGF is only secreted by endothelial cells that contact pericytes. An endothelial cell contacts a pericyte when it shares at least 10% of its membrane with pericytes. We set this, arbitrary, to prevent a few pseudopod extensions from inducing VEGF secretion.

chemo-attractant	**sensitivity**	**secretion rate** $[s^{-1}]$	**decay rate** $[s^{-1}]$	**diffusion coefficient** $[m^2 s^{-1}]$
MEC	500	10^{-2}	10^{-3}	10^{-13}
MPC	500	10^{-3}	10^{-4}	10^{-13}
VEGF	500	10^{-3}	10^{-3}	10^{-13}
PDGFB	500	10^{-3}	10^{-3}	10^{-13}

Table 3.1: Parameters related to the chemoattractants.

3.2.3 The *in vitro* patterns cannot be reproduced without endothelial-pericyte signaling

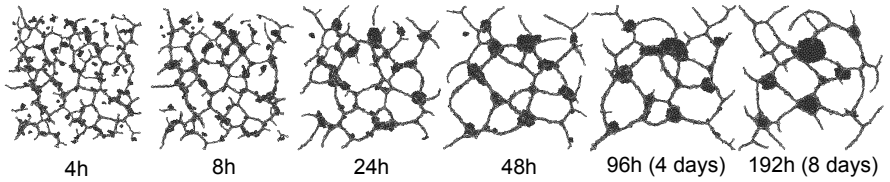

Figure 3.5: Evolution of a simulation with 400 endothelial cells (light) and 200 pericytes (dark).

Before we tested the endothelial-pericyte signaling scenarios, we first tested if any of these interactions are needed to reproduce the patterns that formed *in vitro*. Therefore, we simulated a mixture of elongated endothelial cells and round pericytes at a 2:1 ratio, which is the same ratio as used in the endothelial-pericyte cocultures. Figure 3.5 and Movie S3 show how the morphology of this mixture evolved. The first 8 hours a network develops similar to endothelial-pericyte coculture. But, after one day pericytes clustered at the branch points. This clustering continued, resulting in couple of branch points with large pericyte clusters. Thus, without signaling between endothelial cells and pericytes, a network formed quickly, but the network did not collapse as did happen in the cocultures. This suggests that additional endothelial-pericyte interactions are needed to induce a network collapse.

3.2.4 Heterotypic, chemotactic endothelial-pericyte attraction can cause network collapse

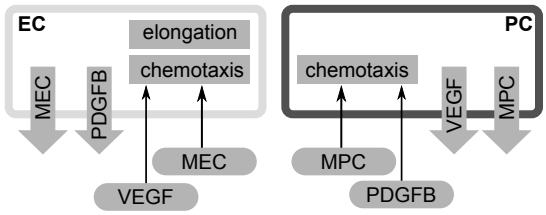

Figure 3.6: Schematic representation of paracrine signaling between pericytes (PC) and endothelial cells (EC). Pericytes secrete VEGF that attracts endothelial cells and endothelial cells secrete PDGFB that attracts pericytes.

In the previous section we combined elongated endothelial cells and round pericytes in one model without endothelial-pericyte signaling. With this model we could reproduce the network formation, but not the network collapse that

occurred in the *in vitro* coculture. This suggests that an additional mechanism is necessary for network collapse. Therefore, we added attraction between endothelial cells and pericytes via chemotaxis to the model. In this section we test the paracrine endothelial-pericyte signaling scenario. In this scenario endothelial cells secrete PDGFB, attracts pericytes, and pericytes secrete VEGF, which attract endothelial cells (Figure 3.6). How the chemoattractants affect pattern formation with endothelial cells and pericytes depends on the secretion rate and the strength of the chemotactic sensitivity of the cells, and the diffusive properties of the chemoattractants. Because VEGF and PDGFB represent generic chemoattractants that attract endothelial cells or pericytes, the values of these parameter are unknown. Therefore, we varied the values of these parameters in our model to elucidate what patterns can form.

First, we explored how the secretion rates of VEGF and PDGFB, and the diffusive properties of VEGF and PDGFB affect pattern formation of endothelial cells and pericytes. To this end we varied secretion and decay rates of VEGF relative to those for PDGFB. All other chemoattractant parameters remained unchanged and are listed in Table 3.1. By keeping the diffusion coefficients constant while varying the decay rate we aim to vary the diffusion length. However, this is only correct when the PDEs describing the concentrations are solved until equilibrium during one time step. We choose the ranges of relative secretion and decay rates such that the PDE solver produced a stable solution and no other modeling artifacts were observed. Figure 3.7**A**-**P** shows the morphologies that formed for varying ratios of secretion and decay. In this figure we recognized three patterns: 1) a network with blobs of pericytes at the nodes (Figure 3.7**A**, **B**, **E**-**G**, **I**-**K**, and **M**-**P**), 2) a nearly collapsed network (Figure 3.7**C**), and 3) cells at the lattice borders (Figure 3.7**D**, **H**, and **L**). The first pattern is similar to the patterns formed without PDGFB or VEGF. Thus, for those secretion and decay rates, PDGFB and VEGF have little effect. The second pattern shares some features with our *in vitro* observations. The cells do aggregate, but the network never fully collapsed (Figure 3.7**Q** and Movie S4). The third pattern does not represent realistic pattern formation. For these simulations the high VEGF secretion of pericytes causes endothelial cells to be more attracted to the pericytes than to other endothelial cells. Therefore, branches of aligned endothelial cells do not become stable, but endothelial cells leave the branch and migrate outwards together with the pericytes. Eventually, most of the cells become stuck at the border of the lattice.

Next, we explored the effects of the chemotactic sensitivity of pericytes to PDGFB and endothelial cells to VEGF. For this we choose a decay and secretion rate for VEGF such that the network collapsed, which are the parameter values used for Figure 3.7**C** ($\varepsilon(\text{VEGF}) = 10^{-5}\text{s}^{-1}$ and a $\alpha(\text{VEGF}) = 10^{-3}\text{s}^{-1}$). The

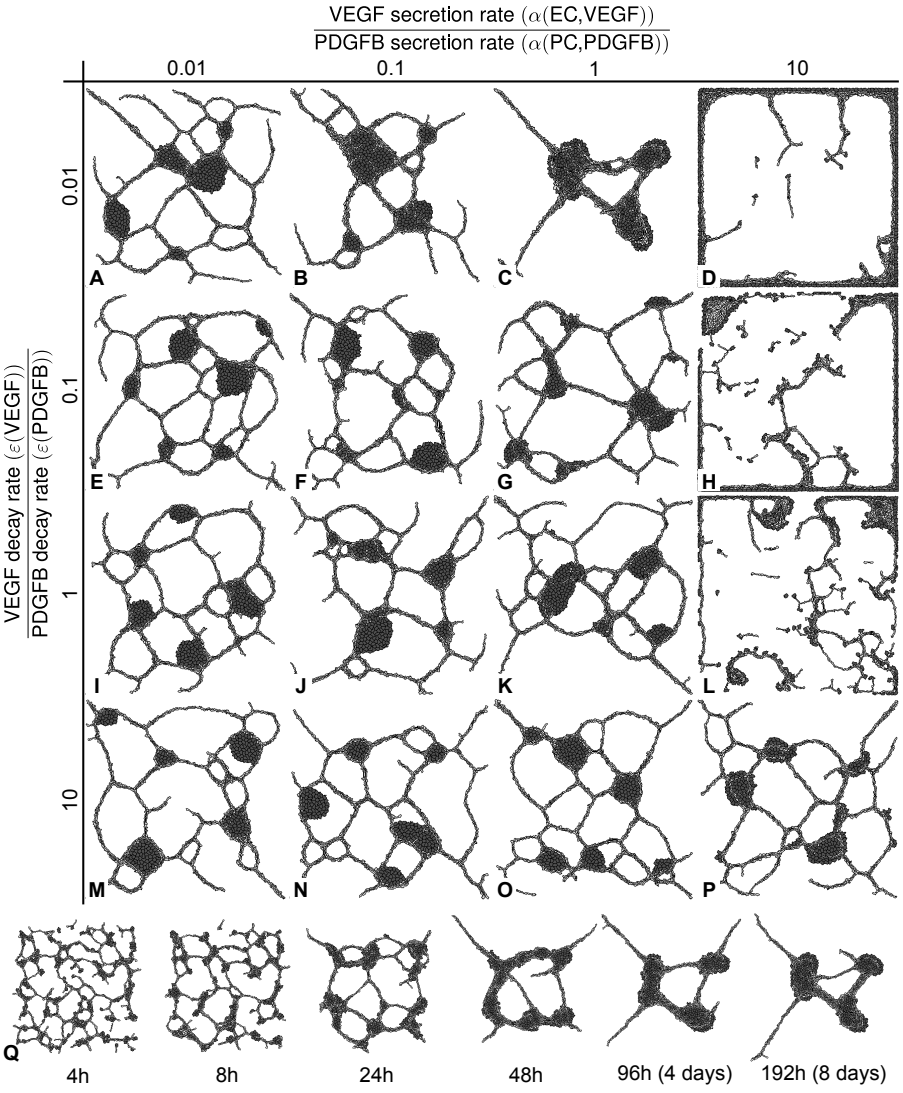

Figure 3.7: **A-P** Patterns formed after ∼192 hours with round pericytes (dark gray) and long endothelial cells (light gray) with varying ratios of PDGFB and VEGF secretion, and varying ratios of PDGFB and VEGF decay. Endothelial cells are attracted to VEGF that is secreted by pericytes and pericytes are attracted to PDGFB that is secreted by endothelial cells (Figure 3.6). **Q** Evolution of pattern in **C**.

range of chemotactic sensitivity was chosen such that chemotaxis affect the patterns, *i.e.* the morphologies differ from those without endothelial-pericyte signaling, and such that there are no model artifacts. Figure 3.8 shows how the final patterns formed with varying chemotactic sensitivity for PDGFB and VEGF. In this morphospace we see two different kinds of blobs: 1) blobs with pericytes on the inside and sprouting endothelial cells on the outside, and 2) blobs with endothelial cells on the inside and pericytes on the outside. The first kind of blobs are stationary, while the second kind of blobs move towards the pericytes. This happens because the chemotaxis of endothelial cells towards VEGF pushes the pericytes ahead. As a result, the cell blobs migrate to the lattice borders where they get stuck.

Altogether, we found that attraction between pericytes and endothelial cells via chemotaxis can affect the patterns these cells form. When VEGF and PDGFB are secreted at the same rate and VEGF diffuses much further than PDGFB, networks formed that collapsed into a blob with long sprouts. Varying the chemotactic sensitivity to VEGF and PDGFB did not improve this collapse. Overall, with the paracrine signaling scenario we partially reproduced the network collapse observed in the *in vitro* cocultures.

3.2.5 Endothelial cell chemotaxis towards endothelial secreted VEGF enables sprouting after network collapse

We showed that PDGFB secretion by endothelial cells and VEGF secretion by pericyte can cause partial network collapse. However, the network did not collapse completely and no new sprouts were formed, which was observed in the endothelial-pericyte cocultures. Therefore, we tested if the second signaling scenario, contact-dependent signaling, could improve network collapse and enable sprouting. In this scenario endothelial cells can secrete both VEGF, which attracts endothelial cells, and PDGFB, which attracts pericytes. PDGFB is secreted by all endothelial cells, similar to the paracrine signaling scenario. VEGF is only secreted by endothelial cells that are adjacent to pericytes (Figure 3.9). As in the previous section, we tested how the chemoattractant secretion rate and diffusive properties, and the cells' sensitivity to the chemoattractant affects the patterns that the cells form.

First, we tested how the relative decay and secretion rates of VEGF and PDGFB affected pattern formation. The ranges of relative decay and secretion rates were chosen such that there were no modeling artifacts, and such that all observed patterns were included. Figure 3.10**A**-**P** shows the patterns that formed with juxtacrine endothelial-pericyte signaling. For almost all tested secretion and decay rates networks formed with a few groups of pericytes on the networks nodes (Figure 3.10**A** and **B**, and **E**-**P**). A single pericyte cluster evolved for only one parameter setting (Figure 3.10**C** and **Q**, and Movie S5). For one other parameter setting the initial network collapsed into a few

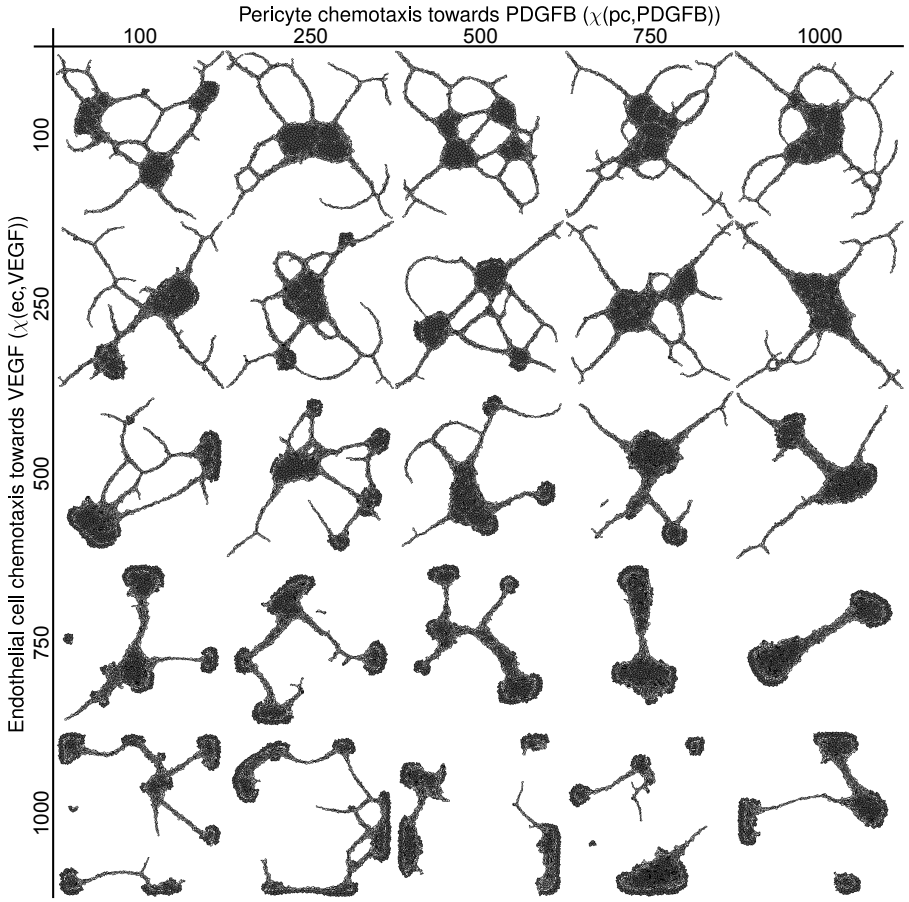

Figure 3.8: Patterns formed after ∼192 hours with 200 round pericytes (dark) and 400 long endothelial cells (light) with varying chemotaxis strengths for pericytes towards PDGFB and endothelial cells towards VEGF after ∼192 hours. Endothelial cells are attracted to VEGF that is secreted by pericytes and pericytes are attracted to PDGFB that is secreted by endothelial cells (Figure 3.6).

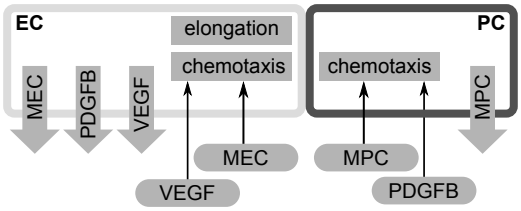

Figure 3.9: Schematic representation of contact-dependent signaling between pericytes (dark) and endothelial cells (light). Endothelial cells secrete PDGFB that attracts pericytes, and endothelial cells that are in contact with pericytes secrete VEGF that attracts endothelial cells.

blobs that later connected via long, thick branches of endothelial cells (Figure 3.10**D** and **R**, and Movie S6). Thus, compared with the paracrine signaling scenario, the contact-dependent signaling scenario did not seem to improve network collapse.

Next, we studied the effects of varying the chemotactic sensitivity of endothelial cells to VEGF and pericytes to PDGFB to test if and how this affects the formed patterns. For this we use a VEGF secretion rate of $10^{-3}s^{-1}$ and VEGF decay rate of $10^{-5}s^{-1}$ because for those settings the network partially collapsed (Figure 3.10**C**). Figure 3.11 shows the patterns that evolved after eight days for varying chemotactic sensitivity towards VEGF and PDGFB. While varying the PDGFB sensitivity of pericytes has little effect on the final morphologies, varying the VEGF sensitivity of endothelial cells had a prominent effect. For a low VEGF sensitivity, a few clusters of pericytes formed inside the network. For higher VEGF sensitivity, a single pericyte cluster formed, from which long branches extended. Interestingly, not all of these branches were part of the initial network. In some simulations new sprouts of endothelial cells extended from the blob (see Figure 3.12 and Movie S7).

Overall, as with the paracrine signaling scenario, for the contact-dependent signaling scenario a blob formed when VEGF had a large diffusion length and was secreted at the same rate as PDGFB. In contrast to the paracrine signaling scenario, here network collapse improved with a higher VEGF chemotaxis. Furthermore, with a higher VEGF chemotaxis new sprouts extended from the collapsed networks. Thus, with the contact-dependent signaling scenario the model reproduced the phenomenology of the endothelial-pericyte cocultures: network collapse and sprout formation.

3.3 Discussion

In this work we studied how pericytes may be involved in angiogenesis using *in vitro* experiments and computational modeling. By including hypothesized

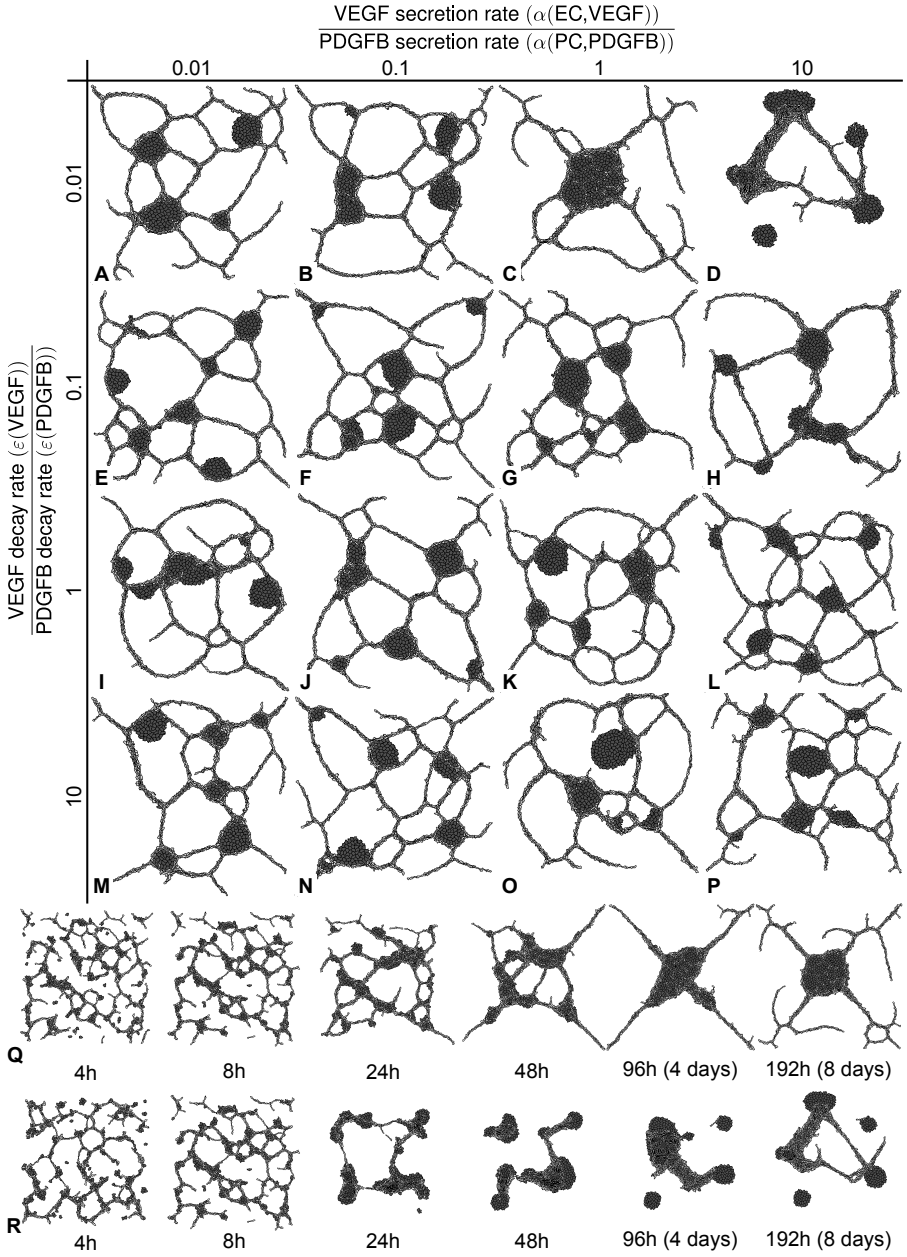

Figure 3.10: **A-P** Patterns formed after ∼192 hours with 200 round pericytes (dark) and 400 long endothelial cells (light) with varying ratios of PDGFB and VEGF secretion, and varying ratios of PDGFB and VEGF decay. Endothelial cells are attracted to VEGF that they secrete when they are in contact with pericytes and pericytes are attracted to PDGFB that is secreted by endothelial cells (Figure 3.9). **Q** evolution of the pattern in **C**. **R** evolution of the pattern in **D**.

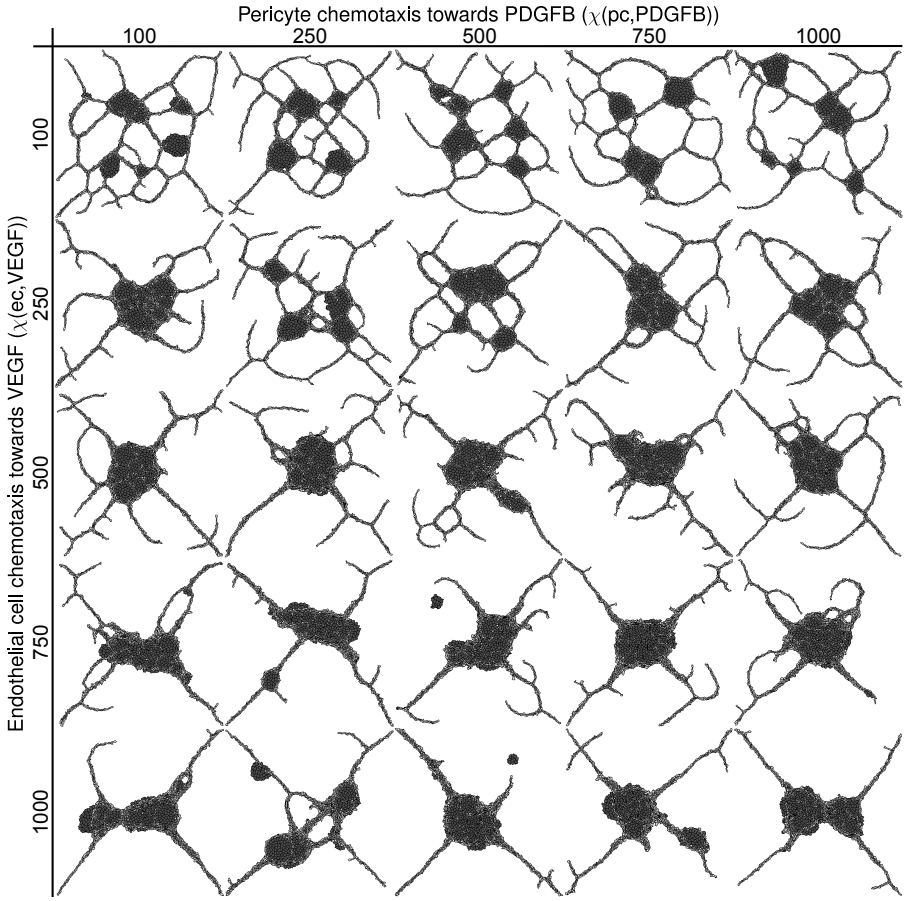

Figure 3.11: Patterns formed after ∼192 hours with 200 round pericytes (dark) and 400 long endothelial cells (light) with varying chemotaxis strengths for pericytes towards PDGFB and endothelial cells towards VEGF. Endothelial cells are attracted to VEGF that they secrete when they are in contact with pericytes and pericytes are attracted to PDGFB that is secreted by endothelial cells (Figure 3.9).

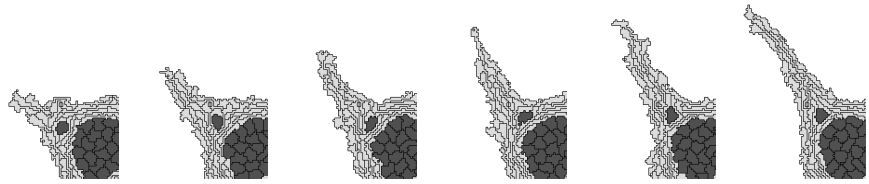

Figure 3.12: New sprout extending from a blob when VEGF is secreted by endothelial cells that are in contact with pericytes. The snapshots were obtained from a simulation with α(EC,VEGF) $= 10^{-3}$), ε(VEGF) $= 10^{-5}$, χ(EC,VEGF) $= 750$, and χ(PC,PDGFB) $= 500$) that ran with 400 endothelial cells and 200 pericytes.

endothelial-pericyte interactions in a computational, cell-based model of angiogenesis we tested which interactions could cause the patterns formed *in vitro*. The experiments showed that pericytes induce a collapse of the network formed by endothelial cells, and endothelial cells induce sprouting in a endothelial-pericyte blob. Based on endothelial-pericyte interactions described in the literature we proposed that endothelial cells and pericytes interact via chemoattractants. With the model we tested two scenarios of endothelial-pericyte signaling: paracrine signaling, and contact-dependent signaling. In the paracrine signaling scenario endothelial cells secreted a chemoattractant for pericytes and vice versa. With this scenario the model reproduced network collapse, but not sprouting. In the contact-dependent signaling scenario endothelial cells secreted a chemoattractant for pericytes, and when endothelial cells are in contact with pericytes they also secrete a chemoattractant for themselves. With this scenario the model reproduced both network collapse and sprouting. Thus, our model supports the hypothesis that endothelial cells and pericytes interact during angiogenesis by secreting chemoattractants. Furthermore, our model indicates that sprouting after network collapse could be the result of pericyte induced secretion of a endothelial cell chemoattractant by endothelial cells. This fits with the observation by Franco *et al.* [119] that endothelial cells secreted the endothelial cell chemoattractant VEGF when they are in contact with pericytes.

In the model we incorporated generic chemoattractants because there exist multiple candidates for each chemoattractant, including VEGF, PDGFB, TGFβ, and Ang-1. By varying the chemical properties of the chemoattractants, the source and rate of chemoattractant production, and the response of cells to the chemoattractants we characterized the cell behavior and chemoattractant properties needed to reproduce the patterns formed *in vitro*. We found that the endothelial cell chemoattractant should diffuse further than the chemoattractant for pericytes. Furthermore, a strong response of en-

dothelial cells to their chemoattractant improves network collapse. To link these properties to a chemoattractant we need experimental data such a diffusion length and the relative strength of chemotaxis. However, this information is scarce and not available for all the chemoattractants we discussed in the introduction. Therefore, we cannot directly link our model predictions to specific chemoattractants.

Our modeling study indicates that the patterns endothelial cells and pericytes form *in vitro* are the result of chemoattractants secreted by endothelial cells and/or pericytes. This hypothesis should be validated experimentally. Because we do not know the identity of the chemoattractants, we cannot use genetic knockouts, trap the chemoattractants, or block the receptors. Instead, we can use two alternative approaches. First, we can test if chemical gradients do indeed play a role in pattern formation. This can be tested by removing the gradients from the culture, for example by constantly tilting the cultures an by seeding the cells on a substrate to which chemoattractants cannot bind. If pattern formation remains unchanged in such cultures, chemotaxis cannot have caused the patterns. Second, we can compare if the distribution of pericytes and endothelial cells predicted by our model matches with *in vitro* observations. In our model, pericytes form the center of the blob, and endothelial cells form the outer layer and sprouts. By labeling endothelial cells and pericytes with different colors, or even by staining the cultures, the distribution of endothelial cell and pericytes can be compared to the model predictions. A difference between the distribution of cells *in vitro* and in the model indicates that the model contains incorrect assumptions, or misses vital cell behavior.

Because we could not completely reproduce the experimental observations, it is likely that the model is missing essential cell behaviors or endothelial-pericyte interactions. In our model we did not account for proliferation, apoptosis and differentiation, which are, among others, regulated by TGFβ and VEGF. TGFβ affects proliferation and differentiation in both pericytes and endothelial cells [98]. However, opposing effects are ascribed to the two TGFβ receptors Alk-1 and Alk-5. Therefore, TGFβ signaling should be understood at the single cell level before it can be added to a cell-based model. VEGF induces proliferation and inhibits apoptosis in endothelial cells [120]. If pericytes are indeed necessary for the production of VEGF, this would explain why the endothelial cells in the monoculture died. Incorporating VEGF regulation of proliferation and apoptosis in the model could result in apoptosis of endothelial cells in sprouts without pericytes and proliferation in the cell blob. Another aspect that may not be represented with sufficient detail is the shape of pericytes. In the model pericytes are modeled as round cells, while in reality pericytes have long extensions via which they contact multiple endothelial cells. Because these extension allow pericytes to interact with mul-

tiple endothelial cells and sense chemoattractants much further away from the cell body, they could play an important role in the model.

3.4 Methods

3.4.1 *In vitro* vasculogenesis assay

Pattern formation of endothelial cells and pericytes was analyzed with *in vitro* vasculogenesis assays with immortalized human umbilical vein endothelial cells (ECRF) and/or human brain vascular pericytes (HBVP). The HBVP were obtained form CellSystems (Troisdorf, Germany) and the ECRF were provided by Ruud Fontein (Academic Medical Center, Amsterdam). Suspensions of ECRF, HBVP, or ECRF and HBVP at a 2:1 ratio were seeded on Matrigel and endothelial growth media (EGM), obtained from Lonza (Breda, The Netherlands), was added. The assays were incubated at 37 °C for eight days (192 hours). At 4, 24, 48 and 192 hours images of the assays were obtained using phase contrast microscopy.

3.4.2 Cellular Potts model

The cellular Potts model (CPM) [84, 85] represents cells on a regular lattice. Each lattice site $\vec{x} \in \mathbb{Z}^2$ is associated with an index $\sigma \in \mathbb{N}$. Cells are sets of lattice sites with the same $\sigma > 0$ and the remaining lattice sites, with $\sigma = 0$, represent the extracellular matrix (ECM). Cell movement and deformation is modeled by attempts to copy the index of a randomly chosen lattice site $\vec{x}$ to one of its eight nearest neighbors $\vec{x}'$. Whether a copy attempt is accepted depends on the change in the *effective energy* (ΔH) that is associated with the copy:

$$p_{\text{accept}}(\Delta H) = \begin{cases} 1 & \text{when } \Delta H \leq 0; \\ e^{-\frac{\Delta H}{\mu}} & \text{when } \Delta H > 0; \end{cases}$$

where μ denotes the cell motility. During one time step of the CPM, called a Monte Carlo step (MCS), as many of copies are attempted as there are lattice sites.

The effective energy depends on the cell behavior that is prescribed in the model. This cell behavior is prescribed for each modeled cell type, which is identified by $\tau(\sigma) \in \{\text{ECM,EC,PC}\}$. In the standard CPM, the effective energy includes cell adhesion and area conservation:

$$H = \underbrace{\sum_{(\vec{x},\vec{x}')} J(\tau,\tau')(1-\delta(\sigma,\sigma'))}_{\text{cell adhesion}} + \underbrace{\sum_{\sigma} \lambda_A(\tau)\left(a(\sigma)-A(\tau)\right)^2}_{\text{area conservation}}.$$

Cell adhesion depends on the cost $J(\tau,\tau')$ of an interface (x,x') between types τ and τ', with $\sigma = \sigma(\vec{x})$, $\tau = \tau(\sigma(\vec{x}))$, $\sigma' = \sigma(\vec{x}')$ and $\tau' = \tau(\sigma(\vec{x}'))$.

Area conservation is modeled by comparing the actual area $a(\sigma)$ with the target area of that cell $A(\tau(\sigma))$. How much the actual cell area fluctuates around the target area depends on the elasticity parameter $\lambda(\tau)$.

Extra cell behaviors are added by extending the *effective energy* function. For the endothelial-pericyte model we added cell elongation and chemotaxis. To model cell elongation we added a term similar to the area conservation with a target length $l(\sigma)$ an elongation strength $\lambda_L(\tau)$ [25]:

$$H_{\text{elongation}} = \sum_{\sigma} \lambda_L(\tau) \left(l(\sigma) - L(\tau)\right)^2 .$$

The cell length is estimated based on the largest eigenvalue $\lambda_b(\sigma)$ of the cell's inertia tensor: $l(\sigma) = 4\sqrt{\frac{\lambda_b(\sigma)}{a(\sigma)}}$ [121]. To model chemotaxis towards a chemoattractant c we added an extra term to the energy change associated with a copy from $\vec{x}$ to $\vec{x}'$ [90]:

$$\Delta H_{\text{chemotaxis}}(c) = -\max(\chi(\tau, c), \chi(\tau', c)) \left(c(\vec{x}') - c(\vec{x})\right),$$

with $\chi(\tau, c)$ the chemotactic sensitivity of a cell of type τ and chemoattractant c. Because in the model each chemoattractant induces chemotaxis in one cell type, $\max(\chi(\tau, c), \chi(\tau', c))$ is identical to the chemotactic sensitivity of the cell type that responds to c. The concentration of the chemoattractant c is described as:

$$\frac{\partial c(\vec{x}, t)}{\partial t} = D(c)\nabla^2 c(\vec{x}, t) + \alpha(\tau(\sigma(\vec{x})), c) - \varepsilon(c),$$

with $D(c)$ diffusion coefficient of chemical c, $\alpha(\tau(\sigma(\vec{x})), c)$ the secretion rate of c by the cell at $\vec{x}$, $\varepsilon(c)$ the decay rate of c.

All simulations presented in this work were performed on a 400 by 400 pixel lattice, which corresponds with an area of 800 μm by 800 μm. At the start of the simulation 600 cells are randomly distributed on this lattice. For each cell type the CPM parameters as listed in table 3.2 are assigned, which our based on previous work with similar models [25, 28]. Furthermore, all chemoattractant fields are initialized at zero. During the simulation the PDEs describing the fields (Equation 3.4.2) are solved with a forward Euler solver with zero boundaries. The solver runs every MCS with 15 time steps of 2 seconds, thus an MCS corresponds to 30 seconds. To match the duration of the vasculogenesis assays, which is eight days, the simulations must run for 25 000 MCS.

Symbol	Description	Value
J(EC,PC), J(EC,EC), J(PC,PC)	cell-cell adhesion	40
J(EC,ECM), J(PC,ECM)	cell-ECM adhesion	20
A(EC), A(PC)	target area	200 μm^2
λ_A(EC), λ_A(PC)	elasticity parameter	25
L(EC)	target length	60 μm
λ_L(EC)	elongation strength	10
μ(EC), μ(PC)	cell motility	50
χ(EC,MEC), χ(PC,MPC)	chemotaxis	500
χ(EC,VEGF), χ(PC,PDGFB)	chemotaxis	500

Table 3.2: Model parameters describing the behavior of endothelial cells and pericytes.

3.A Supplementary movies

An archive containing all supplementary movies can be found at
`http://persistent-identifier.org/?identifier=urn:nbn:nl:ui:18-22536`

Movie S1 Evolution of a simulation with 600 endothelial cells (light) and no pericytes (Figure 3.4**C**).

Movie S2 Evolution of a simulation with 600 pericytes (dark) and no endothelial cells (Figure 3.4**D**).

Movie S3 Evolution of a simulation with 400 endothelial cells (light) and 200 pericytes (dark) (Figure 3.5).

Movie S4 Evolution of a simulation with paracrine signaling and a low VEGF decay rate (Figure 3.7**C**).

Movie S5 Evolution of a simulation with contact-dependent signaling and a low VEGF decay rate (Figure 3.10**C**).

Movie S6 Evolution of a simulation with contact-dependent signaling and a low VEGF decay rate and a high VEGF secretion rate (Figure 3.10**D**).

Movie S7 New sprout extending from a blob when VEGF is secreted by endothelial cells that are in contact with pericytes. This simulation was performed with 400 endothelial cells and 200 pericytes, and the following parameters: α(EC,VEGF) $= 10^{-3}$), ε(VEGF) $= 10^{-5}$, χ(EC,VEGF) $= 750$, and χ(PC,PDGFB) $= 500$).